

Supporting Information

De Novo Design of a Self-Assembled Artificial Copper Peptide (ArCuP) that Activates and Reduces Peroxide

Suchitra Mitra,^{†,‡} Divyansh Prakash,^{†,‡} Khashayar Rajabimoghadam,[‡] Zdzislaw Wawrzak,[§] Pallavi Prasad,[†] Tong Wu,[‡] Sandeep K. Misra,^{||} Joshua S. Sharp,^{||,†} Isaac Garcia-Bosch,[‡] Saumen Chakraborty^{*,†}

[†]Department of Chemistry and Biochemistry, University of Mississippi, University, MS 38677, USA

[‡]Department of Chemistry, Southern Methodist University, Dallas, TX 75275, USA

[§]Argonne National Laboratory, 9700 S. Cass Ave, Argonne, IL 60439, USA

^{||}Department of Biomolecular Sciences, University of Mississippi, University, MS 38677, USA

Corresponding Author:

*saumenc@olemiss.edu

Author Contributions:

[#]S.M. and D.P. contributed equally.

Table S1. Results from Bcs^{2-} titration to $[\text{3SCC-Cu(I9H)}_3]^+$ in 100 mM MOPS pH 7.5.

| $A_{483\text{nm}}$ | Cu(Bcs)_2^{2-} (μM) | Cu(Pep)_3^{2+} (μM) | $(\text{Pep})_3$ (μM) | $\theta =$ $\text{Cu(Pep)}_3^{2+} /$ $(\text{Pep})_3$ | K_d (M) |
|--------------------|--|--|---------------------------------------|---|-----------------------|
| 0.005 | 0 | 15 | 30 | 0.5 | -- |
| 0.029 | 2.3 | 12.7 | 30 | 0.43 | 5.9×10^{-17} |
| 0.061 | 4.6 | 10.4 | 30 | 0.35 | 2.4×10^{-16} |
| 0.084 | 6.4 | 8.6 | 30 | 0.29 | 6.1×10^{-16} |
| 0.111 | 8.4 | 6.6 | 30 | 0.22 | 1.8×10^{-15} |
| 0.134 | 10.1 | 4.9 | 30 | 0.16 | 5.1×10^{-15} |
| 0.150 | 11.3 | 3.7 | 30 | 0.12 | 1.2×10^{-14} |
| 0.167 | 12.6 | 2.4 | 30 | 0.08 | 3.7×10^{-14} |
| 0.173 | 13.1 | 1.9 | 30 | 0.06 | 6.3×10^{-14} |

Total concentration of $[\text{3SCC-(I9H)}_3] = 30 \mu\text{M}$; $\text{Cu(I)} = 15 \mu\text{M}$; $[\text{Bcs}^{2-}] = 33 \mu\text{M}$.

Table S2. Results of kinetic UV-vis experiments.

| pH | ϵ_{330} ($M^{-1}cm^{-1}$) | ϵ_{387} ($M^{-1}cm^{-1}$) | Initial rate @ λ_{330nm} / s^{-1} | Initial rate @ λ_{387nm} / s^{-1} | ϵ_{350} ($M^{-1}cm^{-1}$) ^a | ϵ_{440} ($M^{-1}cm^{-1}$) ^b | Initial rate @ λ_{350nm} / s^{-1c} |
|-----|---|---|---|---|--|--|---|
| 5.5 | 1.8×10^3 | 8.1×10^2 | 3.4×10^{-5} | 3.6×10^{-6} | 3.08×10^3 | 0.09×10^2 | 1.74×10^{-4} |
| 6.5 | 7.2×10^3 | 2×10^3 | 1.1×10^{-4} | 3.8×10^{-5} | 10.4×10^3 | 2.8×10^2 | 1.6×10^{-4} |
| 7.5 | 6.4×10^3 (11.9×10^3) | 1.4×10^3 (3.68×10^3) | 3.2×10^{-4} (6.83×10^{-4}) | 7.3×10^{-5} (3.59×10^{-6}) | 11.9×10^3 (8.57×10^3) | 5.63×10^2 (0.6×10^3) | 7.2×10^{-4} (1.16×10^{-3}) |
| 8.5 | 5.5×10^3 | 1.1×10^3 | 2.4×10^{-4} | 2.3×10^{-5} | 8.4×10^3 | 0.6×10^2 | 5.32×10^{-4} |
| 9.5 | 5.5×10^3 | 1.3×10^3 | 2.2×10^{-4} | 5.8×10^{-5} | 8.89×10^3 | 1.2×10^2 | 5.3×10^{-5} |

^{a,b,c} in the presence of ascorbate, the values in parenthesis are for $[3SCC-Cu(I9HW28Q)_3]^{2+}$.

Table S3. Relevant spectroscopic parameters for the Trp28Gln mutant.

| Sample | λ_{\max} (nm) ($\epsilon / \text{M}^{-1}\text{cm}^{-1}$) | g_x, g_y | g_z | A_x, A_y (MHz) | A_z (MHz) |
|--|---|------------|-------|---------------------|----------------|
| [3SCC- Cu(I9HW28Q) ₃] ²⁺ | 590 (60) | 2.05 | 2.28 | 117 | 525 |
| [3SCC- Cu(I9HW28Q) ₃] ²⁺ +H ₂ O ₂ | 330(9200) 387(2000) | 2.06 | 2.28 | 84 | 525 |
| [3SCC- Cu(I9HW28Q) ₃] ⁺ +H ₂ O ₂ | 350 (7373) 440(690) | 2.06 | 2.28 | 100 | 507 |

Table S4. X-ray data collection and refinement statistics.

| | |
|---------------------------------------|--|
| Wavelength | 0.9786 |
| Resolution range | 19.63 - 1.45 (1.502 - 1.45) |
| Space group | P 63 |
| Unit cell | a = 39.26 b = 39.26 c = 83.63 α = 90 β = 90 γ = 120 |
| Total reflections | 25414 (2203) |
| Unique reflections | 12796 (1181) |
| Multiplicity | 2.0 (1.9) |
| Completeness (%) | 97.08 (81.29) |
| Mean I/sigma(I) | 10.32 (0.65) |
| Wilson B-factor | 23.10 |
| R-merge | 0.01907 (1.49) |
| R-meas | 0.02697 (2.108) |
| R-pim | 0.01907 (1.49) |
| CC1/2 | 1 (0.384) |
| CC* | 1 (0.745) |
| Reflections used in refinement | 12795 (1043) |
| Reflections used for R-free | 555 (54) |
| R-work | 0.2687 (0.4588) |
| R-free | 0.2945 (0.4711) |
| CC(work) | 0.948 (0.440) |
| CC(free) | 0.941 (0.454) |
| Number of non-hydrogen atoms | 702 |
| macromolecules | 675 |
| ligands | 14 |
| solvent | 13 |
| Protein residues | 95 |
| RMS(bonds) | 0.009 |
| RMS(angles) | 1.26 |
| Ramachandran favored (%) | 100.00 |
| Ramachandran allowed (%) | 0.00 |
| Ramachandran outliers (%) | 0.00 |
| Rotamer outliers (%) | 1.89 |
| Clashscore | 0.72 |
| Average B-factor | 39.90 |

Statistics for the highest-resolution shell are shown in parentheses. Table generated in Phenix.

The structure factors and coordinates are provided in the CIF files.

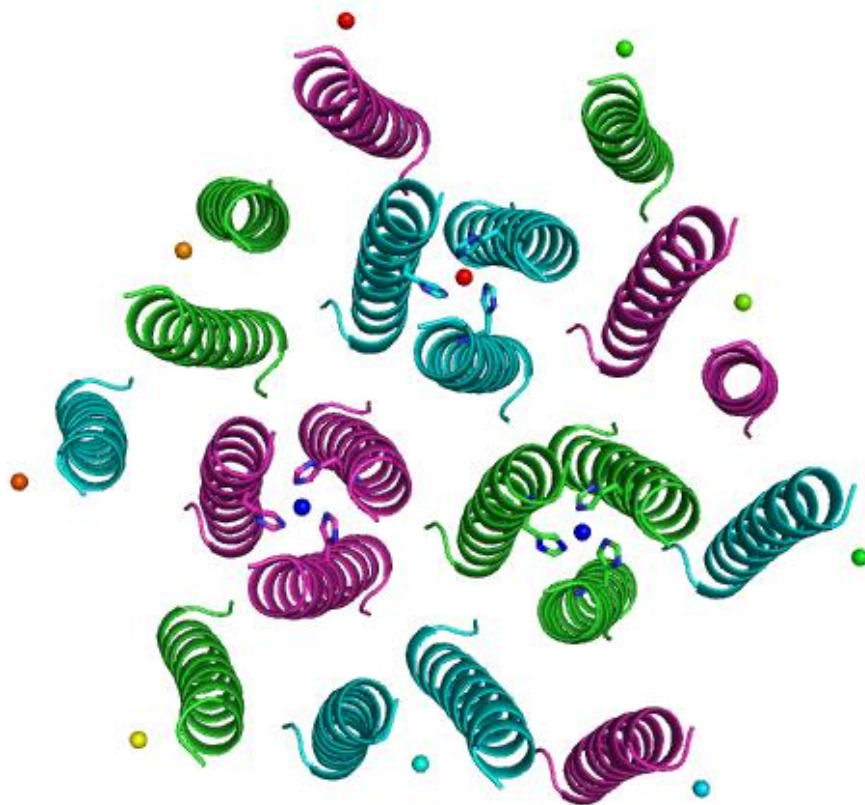


Figure S1. Overall assembly of the ArCuP showing the arrangement of helices. A₃ chains are in green, B₃ chains are in cyan and C₃ chains are in magenta.

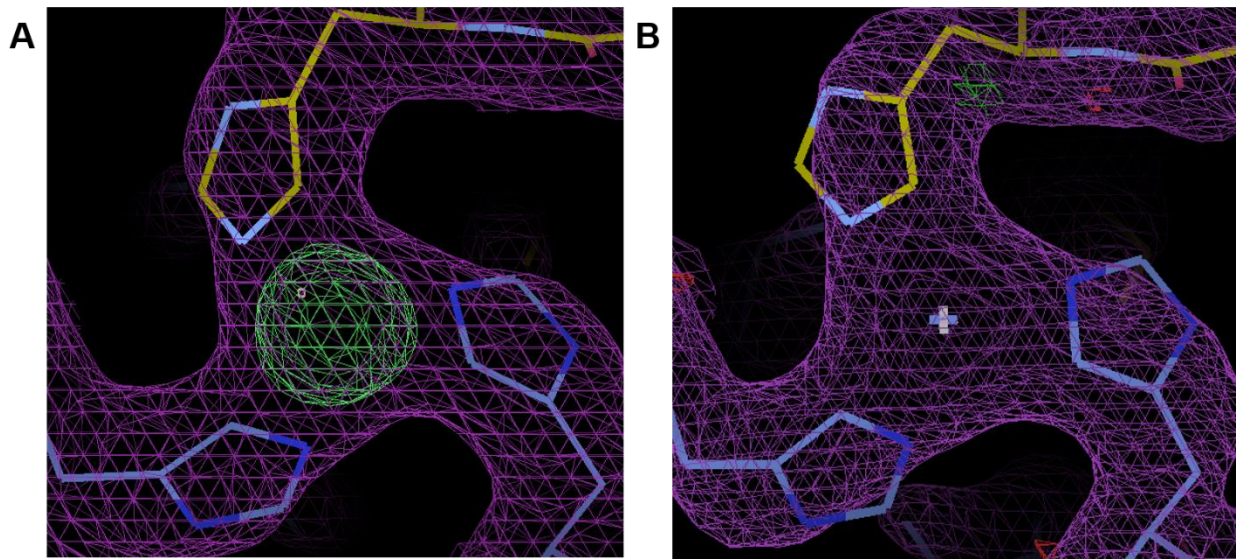


Figure S2. 2F_o-F_c (magenta) and F_o-F_c maps (green) before (A) and after adding Cu followed by refinement (B).

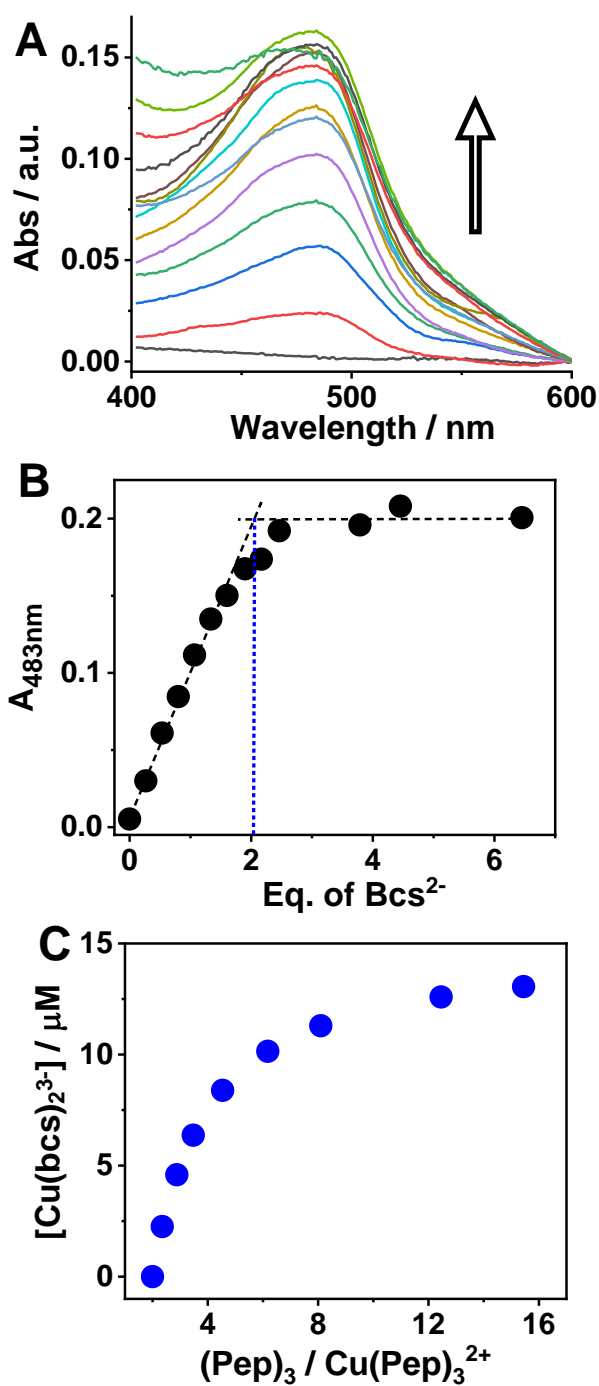


Figure S3. A) Spectra showing the formation of $\text{Cu}(\text{Bcs})_2^{3-}$ during gradual addition of Bcs^{2-} to $[\text{3SCC-Cu}(\text{I9H})_3]^+$ in 100 mM MOPS pH 7.5. B) Plot of A_{483} vs equivalents of Bcs^{2-} showing saturation at 2 equivalents of Bcs^{2-} . C) Plot of $[\text{Cu}(\text{Bcs})_2^{3-}]$ vs $1/\theta$ used to determine $K_d^{\text{Cu(I)}}$. Total $[\text{3SCC}(\text{I9H})_3] = 30 \mu\text{M}$; $\text{Cu}(\text{I}) = 15 \mu\text{M}$; $[\text{Bcs}^{2-}] = 33 \mu\text{M}$. 2-fold excess of free peptide trimer was kept to ensure no free $\text{Cu}(\text{I})$ is present prior to Bcs^{2-} addition.

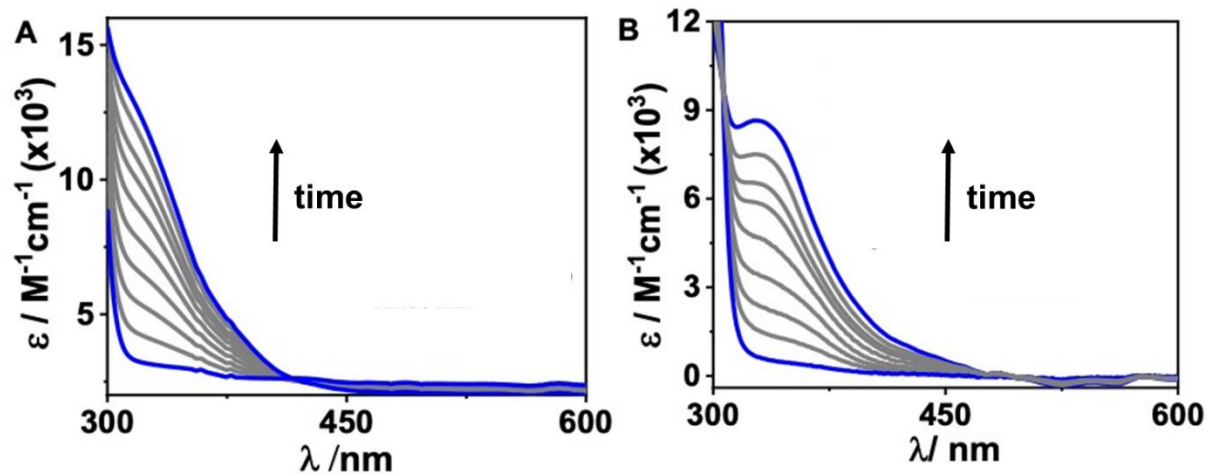


Figure S4. Kinetic UV-vis experiments showing spectral changes observed by addition of 12.5 mM H₂O₂ (final concentration) to 0.125 mM [3SCC-Cu(I9HW28Q)₃]²⁺ (A) and [3SCC-Cu(I9HW28Q)₃]⁺ (B) in 100 mM HEPES pH 7.5.

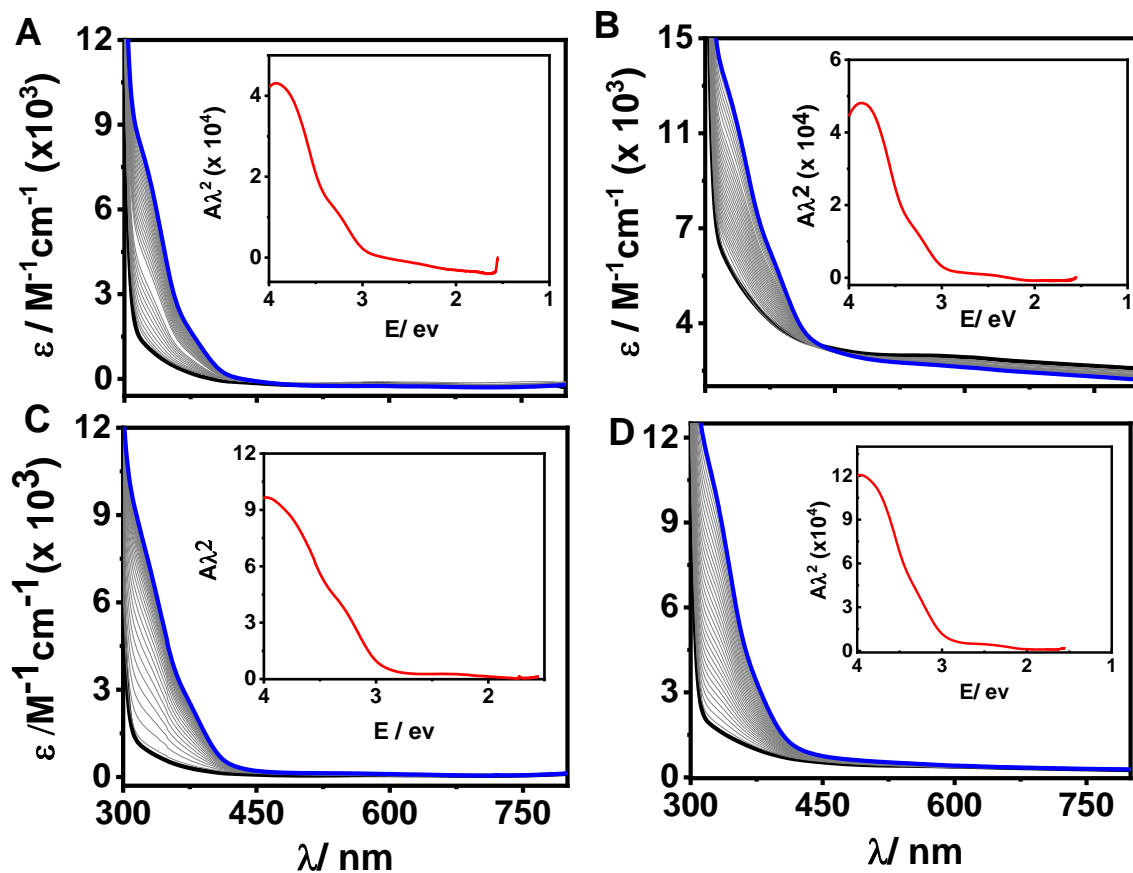


Figure S5. Kinetic UV-vis experiments showing spectral changes observed by addition of 12.5 mM H_2O_2 (final concentration) to 0.125 mM $[\text{3SCC-Cu}(\text{I9H})_3]^{2+}$ in pH 5.5 (A), 6.5 (B), 8.5 (C), and 9.5 (D) in mixed buffers. The initial traces prior to H_2O_2 addition are in black and the final traces after ~ 2 h of H_2O_2 reaction are in blue. The insets show the corresponding energy plots of the final species after H_2O_2 reaction.

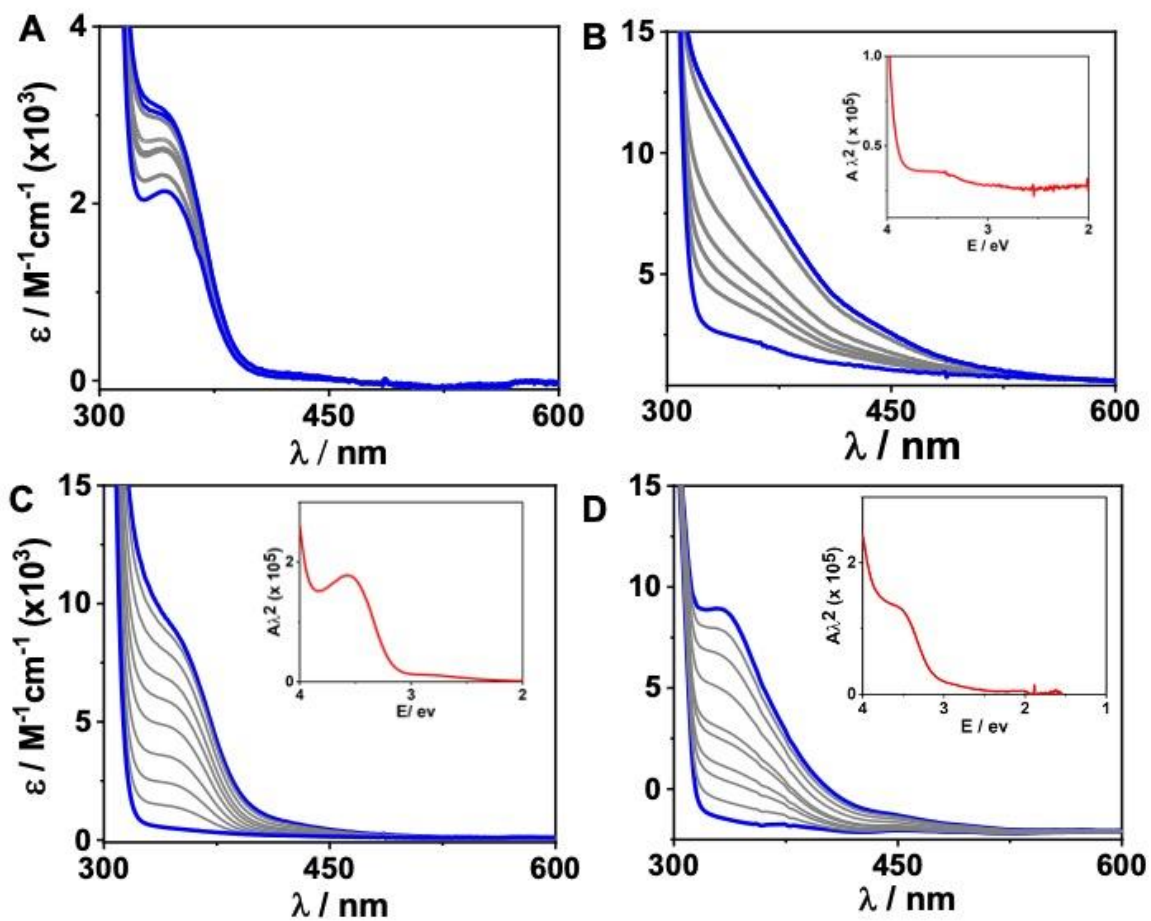


Figure S6. Corresponding experiments similar to Figure S5 but with the Cu(I)-peptide. Experiments are performed under anaerobic conditions to avoid O_2 competition. The insets show the energy plots of the final species after H_2O_2 reaction.

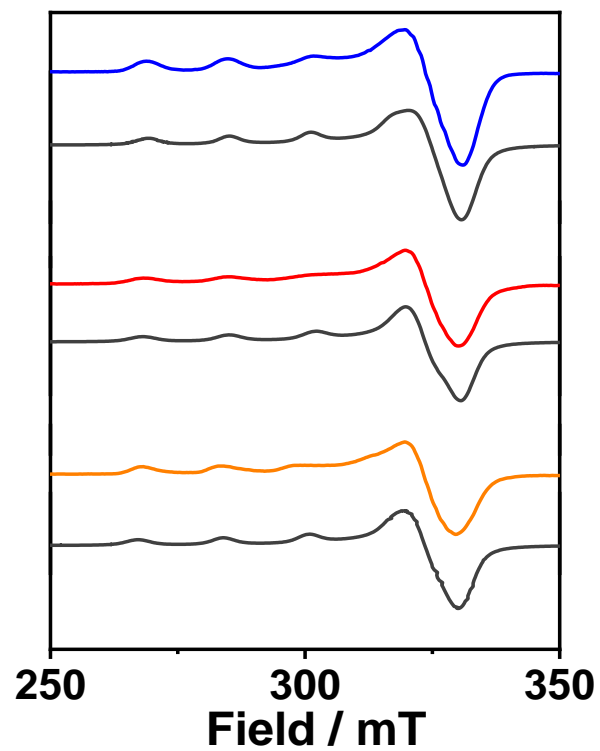


Figure S7. X-band EPR spectra of 0.5 mM $[3\text{SCC-Cu(I9HW28Q)}_3]^{2+}$ (blue), in the presence of 100-fold H_2O_2 (red), and the corresponding Cu(I)-peptide plus H_2O_2 (orange) in 100 mM HEPES pH 7.5. Gray traces are the simulated spectra. All data were collected at 126 K.

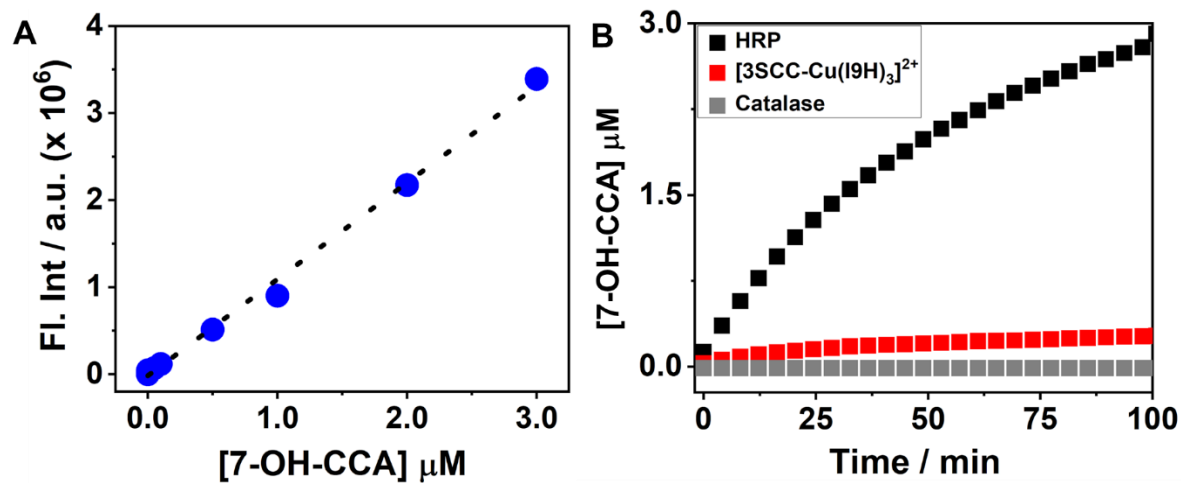


Figure S8. A) Calibration curve for 7-OH-CCA. B) Production of [OH[•]] measured by 3-CCA assay with HRP, catalase, and [3SCC-Cu(I9H)₃]²⁺. Samples contained 0.25 mM proteins, 5 mM 3-CCA, and 25 mM H₂O₂ in 100 mM HEPES pH 7.5. The concentration of 7-OH-CCA in B was calculated from the calibration curve.

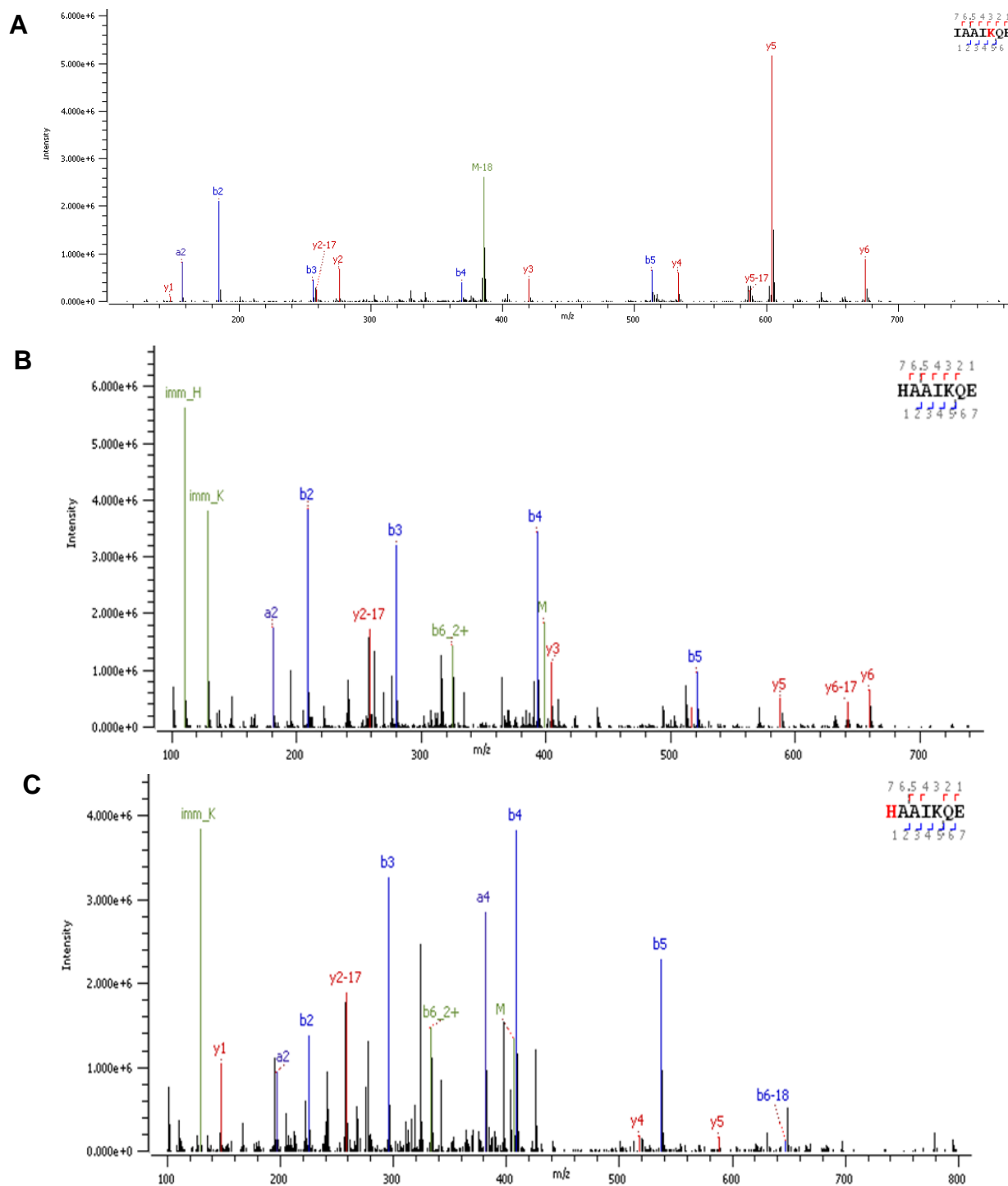


Figure S9. Representative MS/MS spectra of the $[M+2H]^{2+}$ peptide fragment IAAIKQE (A). The HAAIKQE fragments in $[3\text{SCC-Cu}(\text{I9H})_3]^{2+} + \text{H}_2\text{O}_2$ (B), and $[3\text{SCC-Cu}(\text{I9H})_3]^+ + \text{H}_2\text{O}_2$ (C) samples are shown. The *b* and *y* ion series place the oxidation at K5 in (A), and show that His9 is not oxidized in the Cu(II)-peptide (B), while in (C) oxidation of His9 is observed in the Cu(I)-form of the peptide.

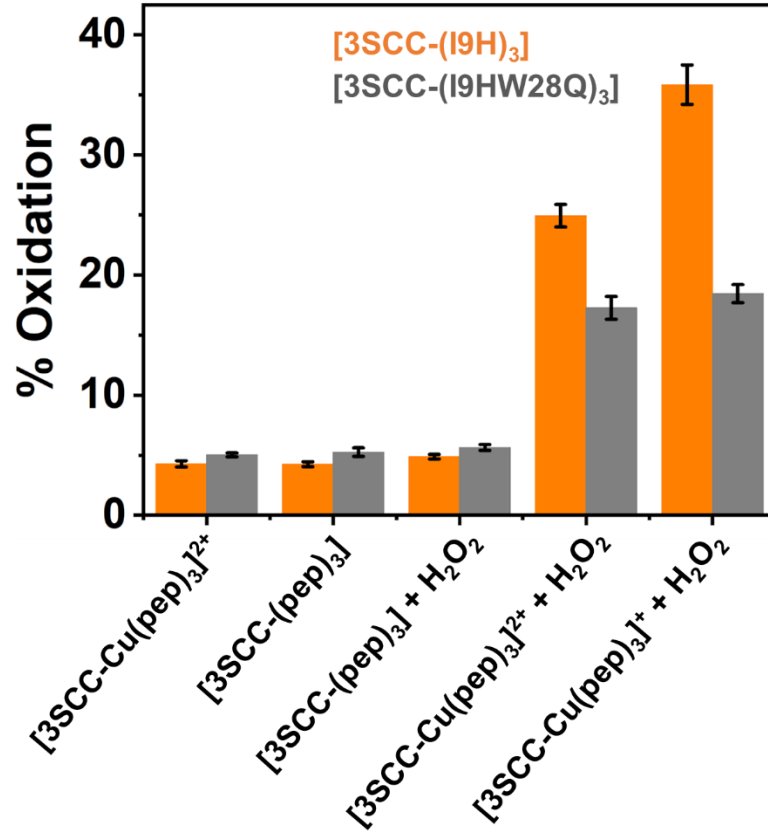


Figure S10. Percent oxidation of the ArCuP (orange bars) and the Trp28Gln mutant (gray bars) under various conditions as investigated by LC-MS/MS. Replacement of Trp28 with Gln results in the decreased oxidation of the peptide. Error bars are from 3 independent sample sets.

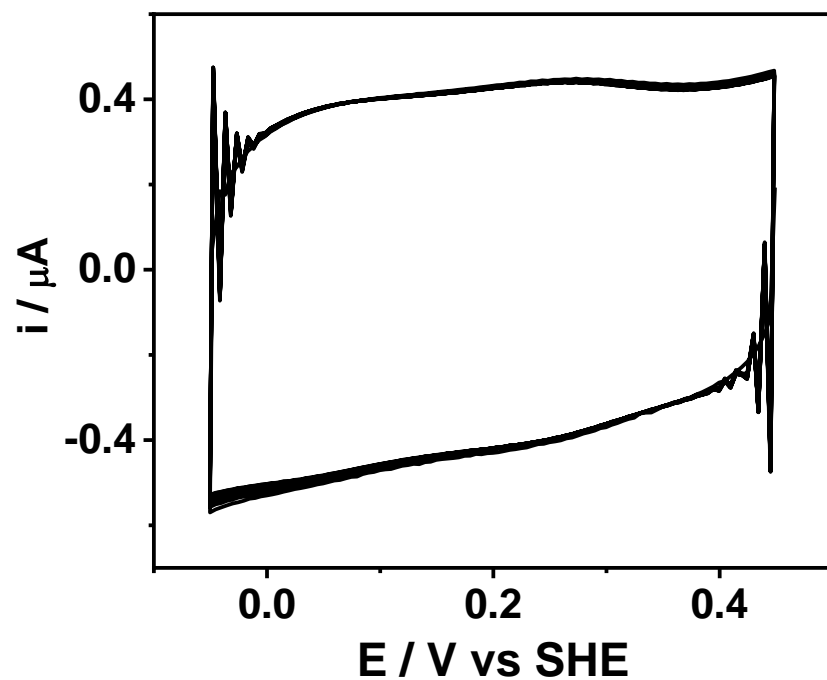


Figure S11. Voltammograms of the ArCuP showing film stability on PGE. Overlay of 30 scans at 20 mVs^{-1} in 80 mM mixed buffer pH 6.5.

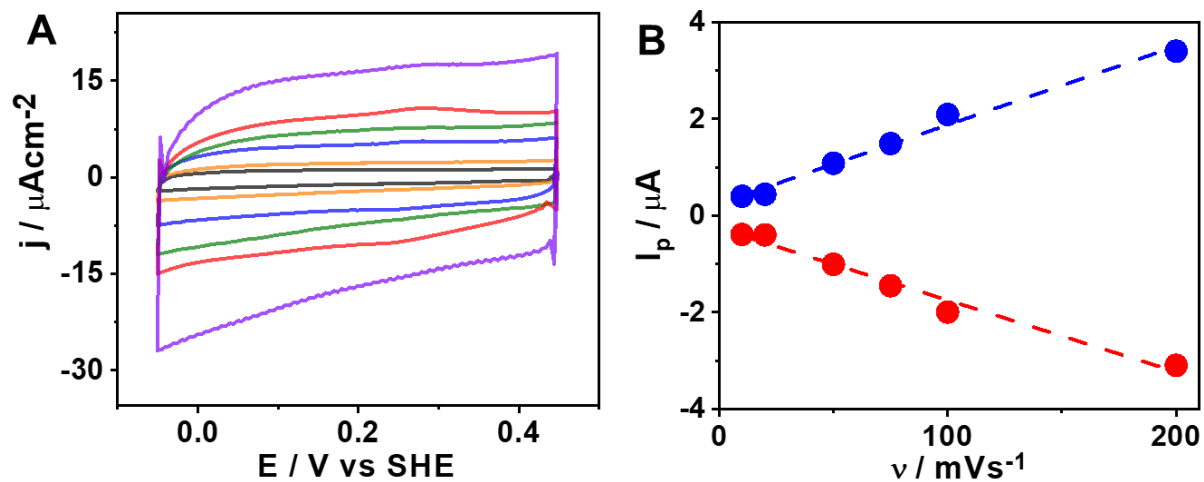


Figure S12. CVs of the ArCuP at $v = 10$ (gray), 20 (orange), 50 (blue), 75 (green), 100 (red), and 200 (violet) mVs^{-1} in 80 mM mixed buffer pH 6.5 (A). The corresponding plot of peak current vs v .

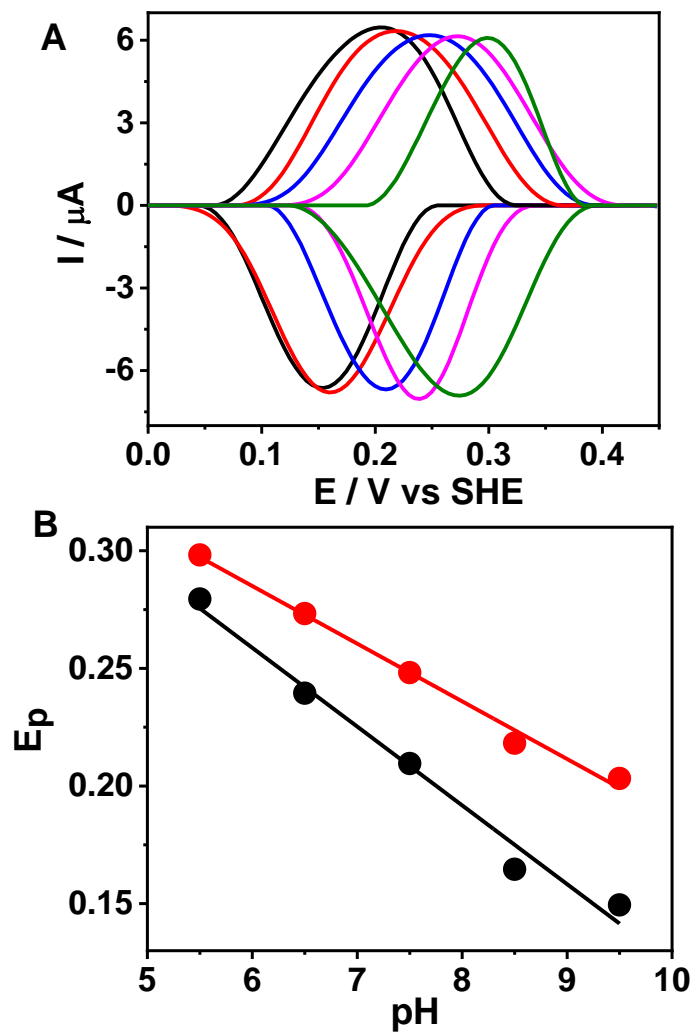


Figure S13. A) Background-subtracted CV scans at pH 5.5 (olive), 6.5 (magenta), 7.5 (blue), 8.5 (red), and 9.5 (black) at 50 mV s^{-1} in 80 mM mixed buffers. B) Plots of anodic (black) and cathodic (red) peak potentials vs pH.

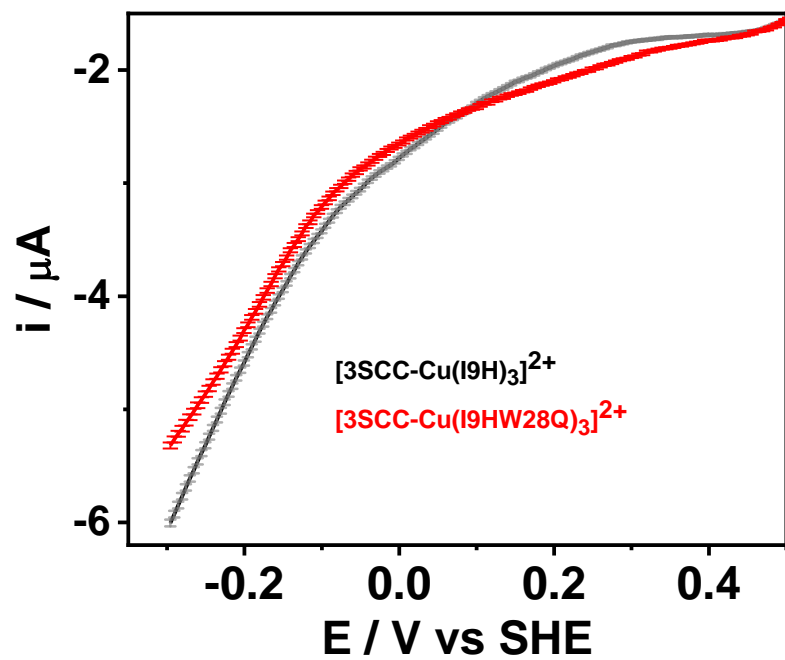


Fig. S14. LSV scans of $[\text{3SCC-Cu(I9H)}_3]^{2+}$ (black) and $[\text{3SCC-Cu(I9HW28Q)}_3]^{2+}$ (red) films on PGE in the presence of 1 mM H_2O_2 in N_2 -saturated 80 mM mixed buffer at pH 7.5.

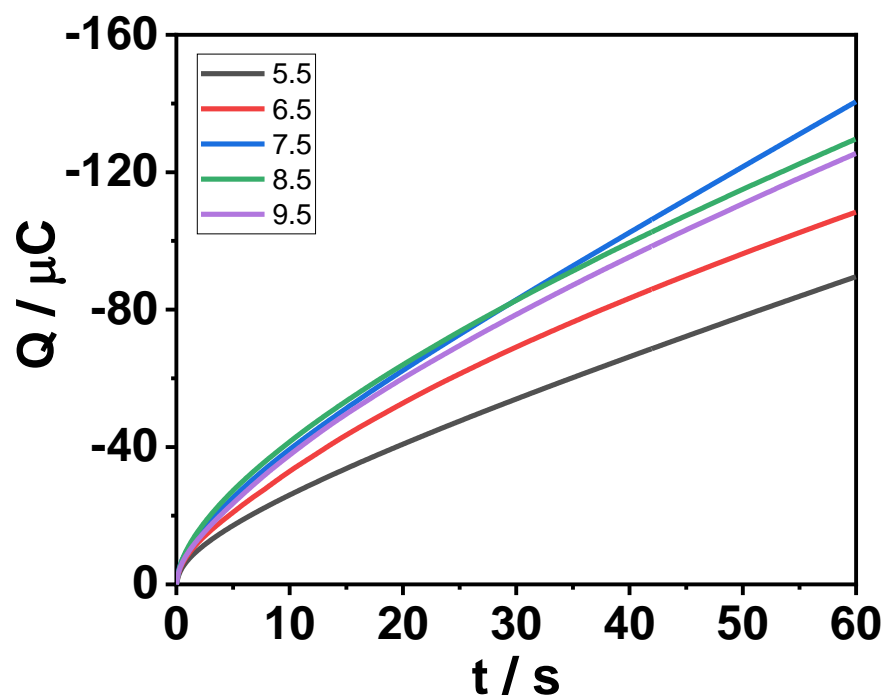


Figure S15. Chronoamperograms of ArCuP films at -0.3V vs SHE at pH 5.5 (gray), 6.5 (red), 7.5 (blue), 8.5 (green), and 9.5 (purple) in 80 mM mixed buffer.

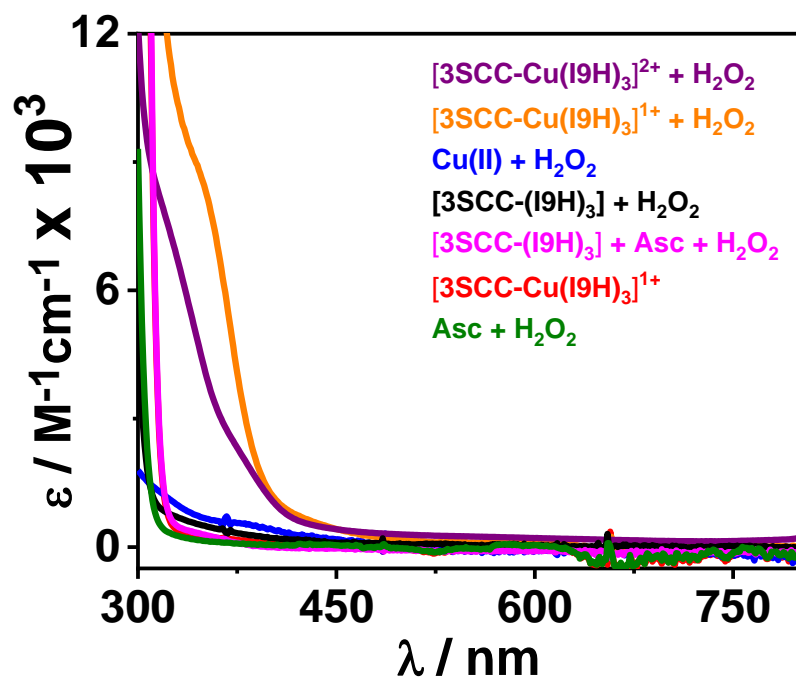


Figure S16. UV-Vis spectra of 0.125 mM $[\text{3SCC-Cu(I9H)}_3]^{2+} + 12.5 \text{ mM H}_2\text{O}_2$ (purple); 0.125 mM $[\text{3SCC-Cu(I9H)}_3]^+ + 12.5 \text{ mM H}_2\text{O}_2$ (orange); free $\text{Cu(II)} + \text{H}_2\text{O}_2$ without the peptide (blue); apo peptide + H_2O_2 (black); apo peptide + $\text{H}_2\text{O}_2 + \text{Asc}$ (magenta); $[\text{3SCC-Cu(I9H)}_3]^+$ only (red); and $\text{Asc} + \text{H}_2\text{O}_2$ (green). All data were collected in 100 mM HEPES pH 7.4.

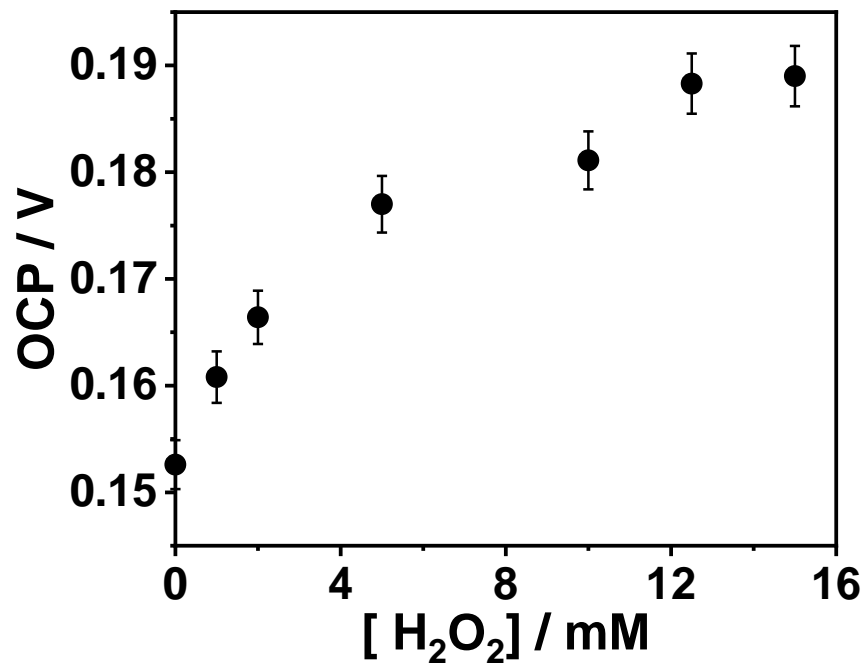


Figure S17. Comparison of OCP values as a function of H_2O_2 concentration at pH 7.5 in 80 mM mixed buffer.

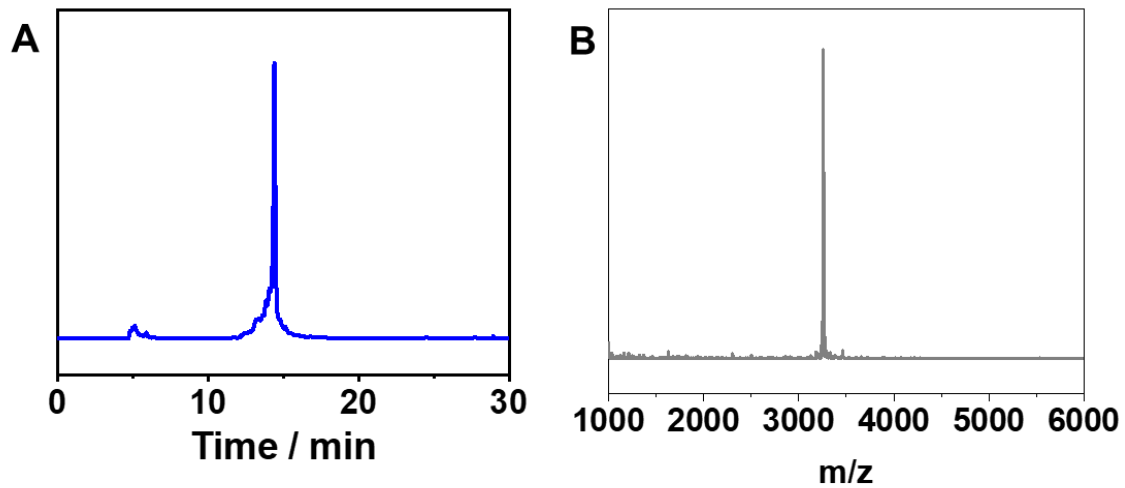


Figure S18. HPLC chromatogram (A) and MALDI-MS (B) spectrum of apo peptide during purification.